

Multi categorical of common eye disease detect using convolutional neural network: a transfer learning approach

Abu Kowshir Bitto, Imran Mahmud

Department of Software Engineering, Daffodil International University, Dhaka, Bangladesh

Article Info

Article history:

Received Mar 21, 2022

Revised May 15, 2022

Accepted Jun 28, 2022

Keywords:

Eye disease

Inception v3

ResNet50

Transfer learning

VGG16

ABSTRACT

Among the most important systems in the body is the eyes. Although their small stature, humans are unable to imagine existence without it. The human optic is safe against dust particles by a narrow layer called the conjunctiva. It prevents friction during the opening and shutting of the eye by acting as a lubricant. A cataract is an opacification of the eye's lens. There are various forms of eye problems. Because the visual system is the most important of the four sensory organs, external eye abnormalities must be detected early. The classification technique can be used in a variety of situations. A few of these uses are in the healthcare profession. We use visual geometry group (VGG-16), ResNet-50, and Inception-v3 architectures of convolutional neural networks (CNNs) to distinguish between normal eyes, conjunctivitis eyes, and cataract eyes throughout this paper. With a detection time of 485 seconds, Inception-v3 is the most accurate at detecting eye disease, with a 97.08% accuracy, ResNet-50 performs the second-highest accuracy with 95.68% with 1090 seconds and lastly, VGG-16 performs 95.48% accuracy taking the highest time of 2510 seconds to detect eye diseases.

This is an open access article under the [CC BY-SA](https://creativecommons.org/licenses/by-sa/4.0/) license.



Corresponding Author:

Abu Kowshir Bitto

Department of Software Engineering, Daffodil International University

Dhaka-1207, Bangladesh

Email: abu.kowshir777@gmail.com

1. INTRODUCTION

According to the world health organization in the world, 2.2 billion people suffer from vision problems. Among the most important organs and systems is the eye. Humans, despite their small stature, are unable to see the surrounding life without it. The white part of the eye, commonly known as the sclera, turns red because of the dilatation of blood vessels [1]. There are several eye diseases. Because the visual system is the standout amongst the most imperative sense organs, it is necessary to detect external eye diseases early. Several studies were done to classify one or more eye disorders, with varying levels of accuracy attained depending on the preprocessing and classification approaches utilized [2]. The human eye is a light-sensitive organ that permits vision. The brain uses information from the eyes to generate perceptions of color, shape, depth, movement, and other characteristics. The sensory nerve system includes the eye.

Conjunctivitis is one kind of eye disease. Conjunctivitis sometimes referred to as pink eye, is an inflammatory disorder of the conjunctiva. Conjunctivitis is a translucent thin layer that daub the eye. The white area of the eye borders the eyelids [3]. It's a rather regular occurrence among kids. It's highly contagious, although it's rarely fatal. It's quite unlikely that it will affect your eyesight. Viral conjunctivitis, bacterial conjunctivitis, and allergic conjunctivitis are the three most common conjunctivitis [4]. Each type of conjunctivitis has its own set of symptoms. As viral conjunctivitis can develop alongside the symptoms of a cold, flu, or other respiratory infection, it is important to get medical attention as soon as possible. Within

several days, it normally starts inside one eye and progresses to another. The most prevalent anterior inflammatory diseases of the eye are allergic conjunctivitis [5]. Allergic conjunctivitis is a kind of allergic conjunctivitis that affects both eyes. Itching, weeping, and swelling of the eyes are possible side effects. Allergy symptoms, such as a runny nose, sneezing, a scratchy throat, or asthma, may develop.

Cataract is one of the eye diseases. Cataract is an obscuring of the eye's lens that root of blindness and vision loss around the world. A cataract is an obscuring of the optic of the eye, which is typically clear. Most cataracts develop gradually and initially have little effect on vision. Cataracts will ultimately obstruct eyesight. Cataract eyes have a few signs and symptoms. Increasing trouble with eyesight at night, clouded, blurred, or dim vision, light sensitivity, glare, color fading or yellowing, double vision in one eye, for example. The cloudiness induced by a cataract may only damage a tiny portion of the eye's lens, leaving the patient oblivious to any visual loss. As the cataract grows bigger, it clouds the lens and causes light to be distorted.

People all over the world suffer from eye illness, which is a common health concern. Cataract and conjunctivitis are two such disorders. Scientists are now concentrating their efforts on employing image processing to diagnose specific eye ailments. The benefits of superior eyesight include enhanced sports talents, better driving skills, improved learning and understanding, and a higher quality of life. As a result, it's critical to detect eye disorders as soon as feasible. Here, we will use different architectures of convolutional neural networks (CNNs) to detect normal eyes, conjunctivitis eyes and cataract eyes with 2250 eyes data individually 750 for normal eyes, 750 for conjunctivitis eyes, and 750 for cataract eyes.

Hom *et al.* [6] used Pearson χ^2 tests and binary logistic regression in their investigation. A number of 689 participants were recruited at random from such an ambulatory care facility. Patients at optometric offices had their itchiness, dryness, and redness levels categorized based on their ocular history and itchiness, dryness, and redness levels. 194 (28.2%) of the 689 people tested had clinically significant itching, 247 (35.8%) had dry eyes, and 194 (28.2%) had redness (28.2%). 112 (57.7%) of the 194 patients with itching had also clinically relevant dryness. 112 (45.3%) of the 247 sufferers with wilted optic had clinically notable irritation. 120 of the 194 individuals with itch (61.9%) and 122 of the 247 individuals with dryness had redness (49.4%). There is a high correlation between redness, dryness, and self-reported irritation. Sambursky *et al.* [7] work with RPS Adeno Detector, immunofluorescence staining for confirmation, and polymerase chain reaction. The cell culture with confirmatory immunofluorescence assay (CC-IFA) method was 91% more sensitive and 100% more specific than polymerase chain reaction (PCR). Triwijoyo *et al.* [8] apply CNN on STARE, which contains 400 retinal color photographs in 24-bit RGB format with a resolution of 605×700 pixels. An ophthalmologist evaluated 200 retinal imaging files. According to the network configuration used, the highest test accuracy of the given picture with the lowest motion of 31×35 pixels is 80.93%. Fourcade *et al.* [9] provide a systematic literature review published in 2019 that was CNNs for health care picture analysis.

The most extensively used CNNs, such as AlexNet and GoogleNet, which were constructed for natural image processing, have proven to be useful for medical imaging. Li *et al.* [10] used CNN and an auto-encoder model. There are two groups in the conjunctivitis dataset. There are 626 photographs in the first group, including 464 healthy images (230 HR and 236 H) and 197 sick images. The second set has 150 photographs, including 100 healthy (50 HR and 50 H) and 50 sick (50 HR and 50 H) images. Sibitz *et al.* [11] analysis of ophthalmology, Chlamydiaceae RT PCR, chlamydiales PCR. 74 cats were used in the study. *C. pneumoniae* has discovered a group of five cats by utilizing Chlamydiaceae RT PCR and subsequent sequence analysis. Two cats having conjunctivitis were found to have *Chlamydia felis*. Prentice *et al.* [12] conducted analytical statistics. Samples were obtained both from the eyes of 104 conjunctivitis-affected neonates and then either the left or right eye of 104 controls, with the side tested matching the conjunctivitis-affected baby. Gaubatz *et al.* [13] work with face recognition, red-eye recognition, and red-eye correction. On a batch of 200 photographs with persons in them, this strategy was put to the test. The technique was able to eradicate roughly 95% of the undesirable red-eye artifacts in the testbed. Jian Wan *et al.* [14] used the active appearance model (AAM). A collection of 300 faceless consumer photos. The technology properly identified roughly 98% of the red-eye anomalies in the test samples. The algorithm missed most of the artifacts since the red eyes were not visible to the naked eye. Verma *et al.* [1] apply CNN. The research utilized 28 different photographs of both healthy eyes and bulbar redness. The aim of this research was to distinguish between red and healthy human eyes based on a newly developed CNN classifier in the shortest possible time. Healthy eyes have a classification accuracy of 94.17, while red eyes have a classification accuracy of 99.99. Wang *et al.* [15] used coherent imaging, deep neural networks with 965 colonies from 15 plates that were not presented during the network training or validation stages were used to blindly assess the system's performance in the early detection of bacterial colonies.

Karahan *et al.* [16] apply the Haar algorithm, deep neural network. There are 16K positive and 52K negative image patches in all. The approach has a higher recall value than the Haar algorithm on both the Fddb and CACD datasets. According to the accuracy rate, the Haar approach is successful in the Fddb dataset. Ahmed *et al.* [17] work with backpropagation with a parabola function based on a linear cyclic learning rate. <https://www.shutterstock.com/> was used to gather 590 samples. categorization accuracy is excellent

(89.83%). Sundararajan *et al.* [18] applied deep-learning convolution neural network, and fuzzy segmentation technique on photographs (600) initially, the value for 1500 was increased in data set two, and then the value for 100 images was increased in data set three. Malik *et al.* [19] apply neural network, decision tree, Naive Bayes, and Random Forest in the data including age, disease history, and clinical observations. The accuracy from the advanced algorithm like neural network and native bayes were less than the predication accuracy of random forest and decision tree algorithm that is over 90 %. Masumoto *et al.* [20] worked with DenseNet201, DenseNet121, VGG19, ResNet50, InceptionV3, Xception, Inception, and ResNetV2 models, the training data was 3700 picture, and the evaluation data was 923 images. With 3,700 photos, the neural network was trained to grade conjunctival hyperemia using the JOAS technique. Manchalwar *et al.* [21] used Oriented Gradient Histogram methods. Two images of cataracts, two images of conjunctivitis, and two images of normal eyes use for data. Used HOG to extract features and a minimum distance classifier was used to categorize the extracted features. Jain *et al.* [22] approach CNN. The initial batch comes from Friedrich-Alexander University's database of machine learning. A total of 15 healthy retinal fundus photographs were taken, as well as 30 ill retinal fundus picture with a mix of diabetic retinopathy and glaucoma. Achieved average accuracy of 96.5% and 99.7% on such datasets. Tsubota *et al.* [23] proposed Hansel's approach. The conjunctivas of 18 patients with vernal and allergic conjunctivitis and 10 patients who served as controls were scrapped.

Dong *et al.* [24] worked with the method of maximal entropy. softmax classifier, CNN, support vector machine. The feature created using deep learning and classified by softmax has a greater accuracy when compared to the classification results. Gunay *et al.* [25] applied stochastic gradient descent, GrabCut, and gray-level co-occurrence matrix. For the training set, used 18 healthy and 12 Ad-Cs eye pictures. Corneal images used with our basic setup and analyzed with the DIP approach proposed successfully detected and isolated possibly infectious patients. They are correct 93% of the time. Bhadra *et al.* [26] used the OpenCV approach developed with a dataset of 100 photos. The procedure of the suggested revolutionary strategy is implemented using the OpenCV library. The accuracy of larger-scale tests can be increased even more by collecting additional dataset photographs. Perdomo *et al.* [27] worked with LeNet convolutional network. The CNN model performs admirably with recognizing exudate in eye fundus images. This research gave encouraging early results in identifying exudate. Hag *et al.* [28] work with gauss gradients, fuzzy method, CNNs. Chakraborty *et al.* [29] use CNN, optical coherence tomography (OCT) and chest X-ray photographs of 1-5-year-old children are assessed and used as inputs. The eye dataset has a validation accuracy of around 90%, while the lung dataset has a validation accuracy of around 63%. Nazir *et al.* [30] used Mask RCNN and Densenet-77 methods. This study was conducted with 650 images, including 168 glaucomatous samples and 482 no glaucomatous samples. The proposed framework's accuracy, recall, F-measure, and IOU were 0.965, 0.963, 0.97, and 0.972. Vigil *et al.* [31] apply YOLO, R-CNN, WordTree, ImageNet, and COCO. There are 9418 classes in the WordTree datasets. The total number of classes in the Imagenet release is 9000. compare the average mAPs of both engines in light of their distinct recognition frameworks to assess their speed and accuracy. With an mAP of 53%, it is twice as fast as any other known model for object detection. Using 63%, YOLO keeps up with the pace. Prasad *et al.* [32] develop a graphical user interface for CNNs. The Glaucoma datasets were got from Medimrg, while the DR dataset was obtained from Kaggle. The rate of accuracy was set at 80%. Using parameter tuning and cross-validation procedures. Nsaif *et al.* [33] used ResNet-50, faster R-CNN, Gabor filters, and Naive Bayes model. In an open dataset (CASIA-Iris-Distance database, Version 4.0), there are 2,567 UV photos of 142 people with different levels of reflection or blocking by the glass. In our paper, we have applied CNN based transfer learning (TL) models to detect and classify the three types of eye conditions (cataract eye, conjunctivitis eye, and normal eye) and also suggest the best model from our model performance evaluation.

2. RESEARCH METHOD

The methodology model, dataset, data preprocessing, data visualization, and model description are the five sub-sections of this section. The section's specifics are shown below.

2.1. Methodology model

We must go through numerous fundamental procedures, including data gathering, data processing, model implementing, calculating performance, and generating results; the workflow diagram presents in Figure 1. We describe how we collect data in the dataset portion, process the dataset for future use in the data preprocess. We will examine each model's performance and look for eye detect of each class.

2.2. Data description

It is impossible to overestimate the relevance of datasets in machine learning research [34]. The type of competent and meticulous human annotation used in dataset gathering techniques in previous periods was

shunned as the machine learning industry progressively shifted to data-driven methodologies. As ‘slow and costly to acquire’, and a shift toward an unrestricted gathering of ever-larger amounts of data. The use of a large bundle of data from the internet, in addition to a greater dependence on non-expert crowd workers, was seen. Machine learning will benefit from this. In present years, a number of issues have been raised about dataset collecting, annotation, and documentation procedures. We collect data from shutter stock and the google website. Collected 2250 eyes data individually 750 for normal eyes, 750 for conjunctivitis eyes, and 750 for cataract eyes. For future usage, we confirm our data with a medical officer.

During the experimentation, the dataset was taken into consideration. The customized eye disease dataset contains 2250 photos, 1689 of which are for training and the remaining 561 for testing. Many difficulties arose during the data collection process. Visualization of sample data for three class as (a) cataract eyes (b) conjunctivitis eyes and (c) normal eyes, is presented in Figure 2.

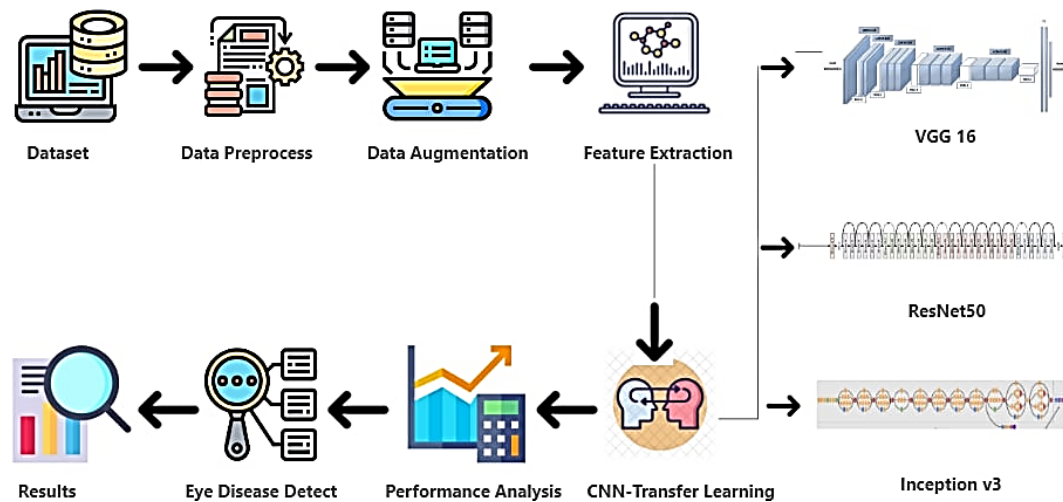


Figure 1. Workflow diagram

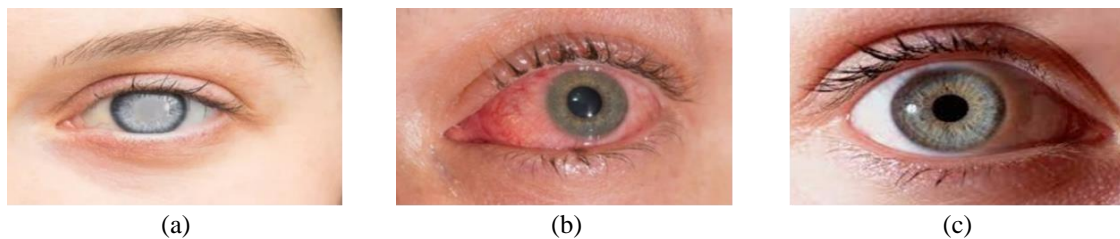


Figure 2. Visualization of sample dataset (a) cataract eyes (b) conjunctivitis eyes and (c) normal eyes

2.3. Data preprocessing

Picture preprocessing improves the efficacy of the image data required for image classification. Geometric alterations are used in preprocessing procedures. Rotation, scaling, and translation of images are all examples of image manipulation. We lowered the resolution of the data during the preparation stages. Based on image alterations, including such rotation, width shifting, height shift, shear shift, and horizontal flipping, were applied to the photos.

2.4. Model theory

The model implementation is the link between the theory and the three TL model (Vgg-16, ResNet-50, and Inception-v3) architecture described underneath.

2.4.1. Retraining a model

Assume that if we want to finish goal 'one' however, there is not enough data to train a deep neural network., we should look for a task 'two' that is similar. That is correct. Use the model as a jumping-off point for solving problems. After training it on 'two,' it faces new hurdles.

2.4.2. Using a pre-trained model

The second alternative is to use a pre-trained method. There are several models available; however, how many layers to adopt and how much retraining to perform depends on the situation. Keras, for example, has nine pre-trained models for computer vision tasks, TL, forecasting, feature extraction, and fine-tuning. In all of these models, we used three pre-trained models: VGG16, ResNet50, and Inception V3.

2.4.3. Transfer learning

TL is the technique of transferring information from one domain to another. Alternative for feature extraction and categorization TL stands for carried out with the use of a deep CNN model that has been in terms of deep learning, it had already been trained on a large dataset. Because fine-tuning a CNN model that has already been trained is usually faster, and considerably less time-consuming than training a CNN model with random data. TL has recently been updated to include weights that have been initialized from the start. The CNN models' initial layers learn characteristics such as edges, the former levels have curves, corners, and color blobs.

2.4.4. Visual geometry group

Visual geometry group (VGG16), is an excellent 16-layer deep vision neural network model. The network receives a two-dimensional image as input (224, 224, 3). The padding on the first two levels is the same, and the first two layers with 64 channels of 33 filter sizes. After, there are two layers with 256 filter size convolution layers, followed by a stride (2, 2) max pool layer (3, 3). A stride (2, 2) max-pooling layer follows, which is identical to the one before it. There are 256 filters in total, as well as 2 convolution layers with 3 filter sizes presented in Figure 3. There are 2 types of 3 convolution layers, as well as a max pool layer. After that, the picture is converted into a two-layer convolution stack. In these convolution and max-pooling layers, 33 filters instead of 1111 filters in AlexNet and 77% in ZF-Net.

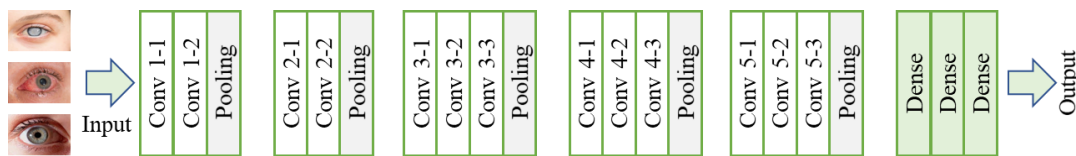


Figure 3. Working procedure of VGG-16 in eye disease detection

2.4.5. Residual networks

Residual network (ResNet50) is a 50-layer CNN. ResNet50 is a 48-layer residual network with one max pool layer and one average pool layer. Each of the ResNet-50 model's 5 phases has its own convolution and identity block presented in Figure 4. There are three convolution layers in each inversion block, and three convolution layers in each identification block. There are around 23,000,000 trainable parameters in the ResNet-50.

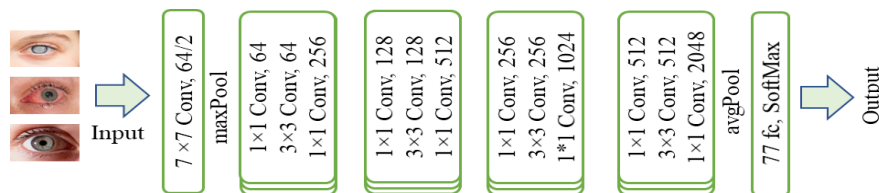


Figure 4. Working procedure of ResNet-50 in eye diseases detection

2.4.6. Inception v3

As a Googlenet module, the Inception-v3 was designed to aid with image processing and object detection. It is Google's Inception CNN latest iteration that made its debut early this year at the ImageNet review and assessment. The goal of Inception-v3 was to improve the service and maintain the number of parameters within control; it has "under 25 million parameters", whereas AlexNet had 60 million. The working procedure diagram of Inception-v3 is present in Figure 5.



Figure 5. Working procedure of Inception-v3 in eye diseases detection

2.5. Model performance calculation

Here are some of the measures for evaluating performance that was calculated. Using these criteria we found the best classifier to detect eye diseases. Many performance indicators in percentage (%) have been calculated using (1)–(7) depend on the confusion matrix stated in [35], and [36] generated by the classifier.

$$Accuracy = \left(\frac{TP + TN}{TP + FN + FP + TN} \right) \times 100\% \quad (1)$$

$$True\ Positive\ Rate\ (TPR) = \left(\frac{TP}{TP + FN} \right) \times 100\% \quad (2)$$

$$True\ Negative\ Rate\ (TNR) = \left(\frac{TN}{FP + TN} \right) \times 100\% \quad (3)$$

$$False\ Positive\ Rate\ (FPR) = \left(\frac{FP}{FP + TN} \right) \times 100\% \quad (4)$$

$$False\ Negative\ Rate\ (FNR) = \left(\frac{FN}{FN + TP} \right) \times 100\% \quad (5)$$

$$Precision = \left(\frac{TP}{TP + FP} \right) \times 100\% \quad (6)$$

$$F1\ Score = \left(2 \times \frac{Precision \times Recall}{Precision + Recall} \right) \times 100\% \quad (7)$$

3. RESULTS AND DISCUSSION

The 1689 training images and 561 validation images of eye disease were sorted into 80:10 groups. An Intel Core i5 processor and 8 GB of memory power the experiment platform. All input photos for the ResNet50, VGG16, and Inception-v3 models were scaled to 224×224, 224×224, and 224×224 respectively. Following that, the augmentation was completed. The weights of the pre-trained VGG-16, ResNet50 finally Inception-v3 models were employed. In Table 1, the generated confusion matrix, (TP, FN, FP, TN) for each of the applied models has been shown with three classes.

Table 1. Confusion matrix for each class with three TL models

Model	Class	TP	FN	FP	TN
VGG-16	Cataract eye	327	19	9	206
	Conjunctivitis eye	268	21	3	269
	Normal eye	311	17	7	226
ResNet-50	Cataract eye	336	22	5	198
	Conjunctivitis eye	347	9	4	201
	Normal eye	309	26	5	221
Inception-v3	Cataract eye	319	10	6	226
	Conjunctivitis eye	289	13	9	251
	Normal eye	304	4	8	245

In VGG-16, we utilized the Adam optimizer with a size of 32 batch and a categorical cross-entropy loss function. The default variables for learning rate, decay, and momentum were utilized in this model. We were able to increase the number of images taken using this method, despite the fact that most earlier attempts had resulted in fewer shots being taken. We're trying to train VGG-16 using 4 epochs, with the objective of having those learning algorithms traverse the whole training data set 20 times. The testing phase begins after the instruction has been given to confirm that the instructions have been followed appropriately. The accuracy of both training and validation are shown in Figure 6(a), while the loss of both training and validation are shown in Figure 6(b). Table 2 shows the performance assessment matrices for the VGG-16 model for each class. Table 2 reveals that the VGG-16 model has a 95.72% accuracy rate for recognizing conjunctivitis eye

illnesses and normal eyes. The best precision for conjunctivitis eye was 98.89%, whereas the maximum F1 score for a normal eye was 96.28%. The maximal sensitivity of the natural eye is 94.82%.

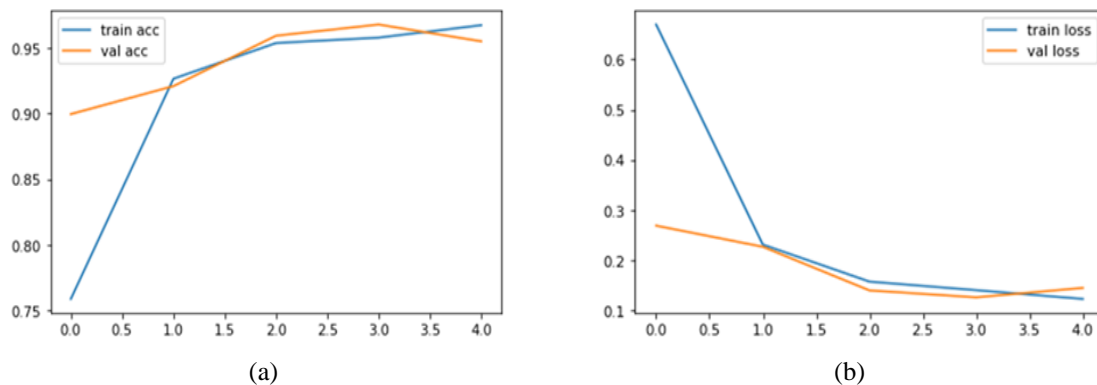


Figure 6. Performance (a) training vs validation accuracy and (b) training vs validation loss for VGG-16

Table 2. Class wise performance evaluation matrices for VGG-16

Model	Class	Accuracy (%)	TPR (%)	FNR (%)	FPR (%)	TNR (%)	Precision (%)	F1 Score (%)
VGG-16	Cataract eye	95.01	94.51	5.49	4.19	91.56	97.32	95.89
	Conjunctivitis eye	95.72	92.73	7.27	1.10	92.76	98.89	95.71
	Normal eye	95.72	94.82	5.18	3.00	93.00	97.80	96.28

The Adam optimizer was used in ResNet50, with a batch size of 64 and a categorical cross-entropy loss function. In this model, the default values for learning rate, decay, and momentum were utilized. Using this strategy, we were able to increase the number of images collected, when most previous attempts had fewer photos taken. We're trying to train our data with ResNet50 utilizing 4 epochs, with the objective of having those learning algorithms traverse the whole training data set 20 times each. Following the instruction, the testing period begins to ensure that the instructions are followed correctly. Figures 7(a) and 7(b) adorn the accuracy of both training and validation, as well as the training and validation loss. Table 3 shows the performance assessment matrices for the ResNet-50 model for each class. Table 3 reveals that the ResNet-50 model has a 97.68% accuracy rate for diagnosing conjunctivitis eye diseases. The highest F1 score and accuracy for conjunctivitis eye were 98.16% and 98.86%, respectively. With a sensitivity of 97.48%, conjunctivitis eye has the highest sensitivity.

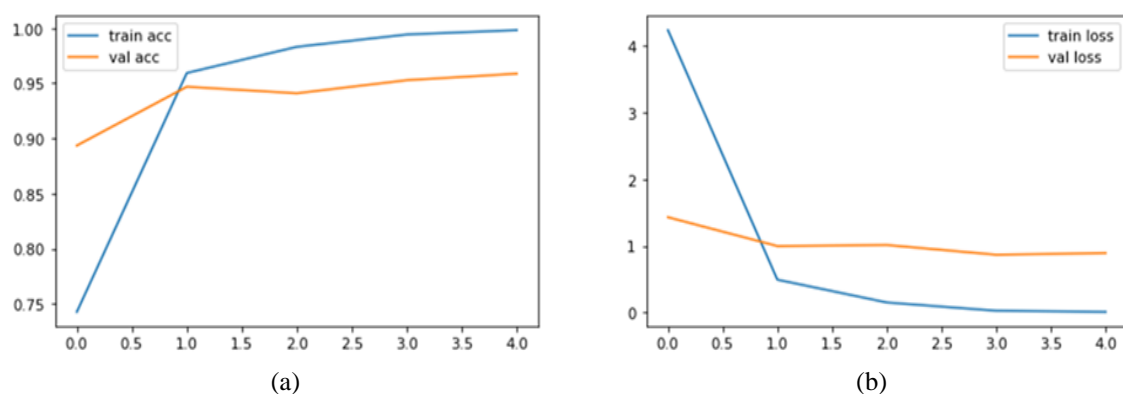


Figure 7. Performance (a) training vs validation accuracy and (b) training vs validation loss for ResNet-50

Table 3. Class-wise performance evaluation matrices for ResNet-50

Model	Class	Accuracy (%)	TPR (%)	FNR (%)	FPR (%)	TNR (%)	Precision (%)	F1 Score (%)
ResNet-50	Cataract eye	95.19	93.85	6.15	2.46	90.00	98.53	96.14
	Conjunctivitis eye	97.68	97.47	2.53	1.95	95.71	98.86	98.16
	Normal eye	94.47	92.24	7.76	2.21	89.47	98.41	95.22

Inception-v3 utilized the Adam optimizer with a batch size of 32 and category cross-entropy as the loss function. The default variables for learning rate, decay, and momentum were utilized in this model. We were able to increase the number of images taken using this method, despite the fact that most earlier attempts had resulted in fewer shots being taken. We're trying to train our data using 5 epochs for Inception-v3, with the objective of having those learning algorithms examine the whole training data set 20 times each. The testing phase begins after the instruction has been given to confirm that the instructions have been followed appropriately. Figures 8(a) and 8(b) adorn the accuracy of both training and validation, as well as the training and validation loss. Table 4 shows the performance evaluation matrices for the Inception-v3 model for each class. The Inception-v3 model has a 97.86% accuracy rate for distinguishing normal eyes, as shown in Table 4. The greatest precision for the normal eye was 98.15%, and the best F1 score for cataract eyes was 98.06. The maximal sensitivity is 98.70% in the typical eye.

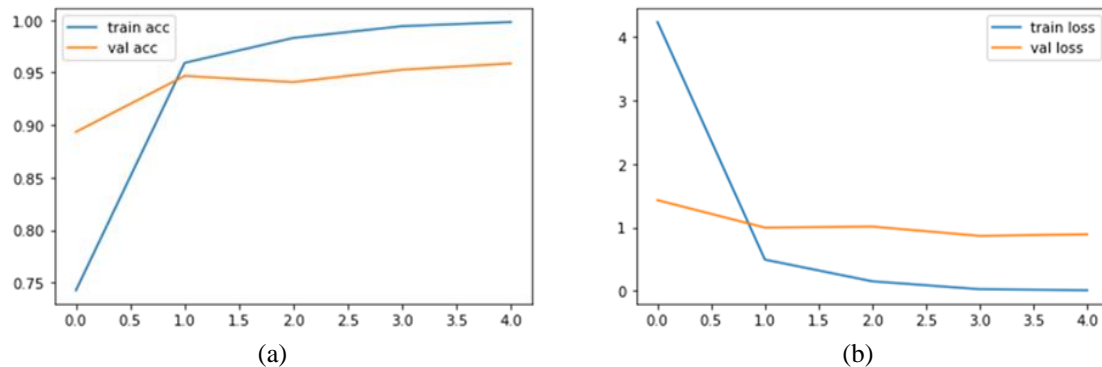


Figure 8. Performance (a) training vs validation accuracy and (b) training vs validation loss for Inception-v3

Table 4. Class wise performance evaluation matrices for Inception-v3

Model	Class	Accuracy (%)	TPR (%)	FNR (%)	FPR (%)	TNR (%)	Precision (%)	F1 Score (%)
Inception-v3	Cataract eye	97.15	96.96	3.04	2.59	95.76	98.15	97.55
	Conjunctivitis eye	96.26	95.70	4.30	3.46	95.08	96.98	96.33
	Normal eye	97.86	98.70	1.30	3.16	98.39	97.44	98.06

In this proposed work, we are attempting to calculate the trained method using the evaluation data set. The training dataset, which included both the original and enhanced photos, was provided to our model as an option for continuing to train. The model was then verified to improve its comprehensiveness. The model's performance was evaluated using test photographs after it was trained on the eye disease dataset using the VGG16, ResNet50, and Inception-v3 architecture. This was done to see how our model stacked up against other well-known TL pre-trained networks. We looked at which pre-trained network will fit this dataset the best. Three separate models, VGG16, ResNet50, and Inception-v3 were examined [37]. From Table 5, we can see Inception-v3 performs the most accuracy with 97.86% with less time 485 seconds, ResNet-50 performs the second-highest accuracy with 95.68% with 1090 seconds and lastly, VGG-16 performs 95.48% accuracy taken highest time of 2510 seconds to detect eye diseases. Table 6 compares our research on detecting eye diseases with those of other authors. With compared to other authors work we used 2250 Images with 3 classes to detect eye disease and we gain 97.08% percent accuracy with Inception-V3.

Table 5. Overall performance evaluation for three TL models

Model	Training accuracy (%)	Training loss (%)	Validation accuracy (%)	Validation loss (%)	Time (s)
VGG 16	96.04	13.21	95.48	14.39	2510
ResNet-50	99.80	0.84	95.78	89.00	1090
Inception-v3	95.86	21.55	97.08	8.81	485

Table 6. Comparative analysis with previous studies

References study	Context	Dataset	No. of class	Best methods	Accuracy (%)
Verma <i>et al.</i> [1]	Classify red and healthy eye	56 images	2	CNN	97.08
Hameed and Ahmed [2]	Eye disease classification	590 images	7	BP-PFLCLR	89.83
Bhadra <i>et al.</i> [26]	Eye disease detection	100	2	OpenCV	87.5
Prasad <i>et al.</i> [32]	Eye disease detection	*NM	2	CNN	80
This study	Multicategorical eye disease detection	2250 images	3	InceptionV3	97.08

*NM: not mention, BP-PFLCLR: back propagation with a parabola function based on a linear cyclic learning rate.

4. CONCLUSION

This study demonstrates the use of TL and deep feature extraction to diagnose eye disease using photographs collected from around the world on the internet. Deep feature extraction and TL are performed using three popular deep CNN architectures: Vgg16, ResNet50, and Inception v3. The gathered dataset is preferable in experimental work because of the high quantity of example photographs. Among all the models Inception-v3 performs the highest accuracy with 97.86% and less time 485 seconds to detect eye disease. ResNet-50 performs the second-highest accuracy with 95.68% with 1090 seconds and lastly, VGG-16 performs 95.48% accuracy taking the highest time of 2510 seconds to detect eye diseases. We plan to utilize different CNN architecture approaches in the future to improve classification precision. Data augmentation for TL will be handled in the future. This research relates to a future goal, such as developing a model that can detect eye disease in real-time approaches such as YOLO. Our findings will aid the medical department in using the technology and detecting eye problems as fast as possible. Mobile devices nowadays offer us convenience and diversity in terms of use. As a result, smartphone cameras could be used to detect eye disease by gathering photographs and videos in a short amount of time, allowing doctors to quickly diagnose and classify eye disease. It will also have a good impact on the growth of a pleasant and secure lifestyle.





REFERENCES

- [1] S. Verma, L. Singh, and M. Chaudhry, "Classifying red and healthy eyes using deep learning," *illumination*, vol. 10, no. 7, 2019, doi: 10.14569/IJACSA.2019.0100772.
- [2] S. Hameed and H. M. Ahmed, "Eye diseases classification using back propagation with parabola learning rate," *Al-Qadisiyah Journal Of Pure Science*, vol. 26, no. 1, pp. 1-9, 2021, doi: 10.29350/jops.2021.26.
- [3] H. M. Ahmed and S. R. Hameed, "Eye Detection using Helmholtz Principle," *Baghdad Science Journal*, vol. 16, no. 4, 2019, doi: 10.21123/bsj.2019.16.4(Suppl.).1087.
- [4] H. M. Ahmad and S. R. Hameed, "Eye Diseases Classification Using Hierarchical MultiLabel Artificial Neural Network," *2020 1st. Information Technology To Enhance e-learning and Other Application (IT-ELA)*, 2020, pp. 93-98, doi: 10.1109/IT-ELA50150.2020.9253120.
- [5] A. Gelincik *et al.*, "Anaphylaxis in a tertiary adult allergy clinic: a retrospective review of 516 patients," *Annals of Allergy, Asthma & Immunology*, vol. 110, no. 2, 2013, pp. 96-100, doi: 10.1016/j.anai.2012.11.018.
- [6] M. M. Hom, A. L. Nguyen, and L. Bielory, "Allergic conjunctivitis and dry eye syndrome," *Annals of Allergy, Asthma & Immunology*, vol. 108, no. 3, 2012, pp. 163-166, doi: 10.1016/j.anai.2012.01.006.
- [7] R. Sambursky, S. Tauber, F. Schirra, K. Kozich, R. Davidson, and E. J. Cohen, "The RPS adeno detector for diagnosing adenoviral conjunctivitis," *Ophthalmology*, vol. 113, no. 10, 2006, pp. 1758-1764, doi: 10.1016/j.ophtha.2006.06.029.
- [8] B. K. Triwijoyo, B. S. Sabarguna, W. Budiharto, and E. Abdurachman, "2-Deep learning approach for classification of eye diseases based on color fundus images," In *Diabetes and Fundus OCT, Elsevier*, pp. 25-57, 2020, doi: 10.1016/B978-0-12-817440-1.00002-4.
- [9] A. Fourcade and R. H. Khonsari, "Deep learning in medical image analysis: A third eye for doctors," *Journal of stomatology, oral and maxillofacial surgery*, vol. 120, no. 4, 2019, pp. 279-288, doi: 10.1016/j.jormas.2019.06.002.
- [10] W. Li, X. Liu, J. Liu, P. Chen, S. Wan, and X. Cui, "On improving the accuracy with auto-encoder on conjunctivitis," *Applied Soft Computing*, vol. 81, 2019, p. 105489, doi: 10.1016/j.asoc.2019.105489.
- [11] C. Sibitz, E. C. Rudnay, L. Wabnegger, J. Spergser, P. Apfalter, and B. Nell, "Detection of Chlamydia pneumoniae in cats with conjunctivitis," *Veterinary Ophthalmology*, vol. 14, 2011, pp. 67-74, doi: 10.1111/j.1463-5224.2011.00919.x.
- [12] M. J. Prentice, G. R. Hutchinson, and D. Taylor-Robinson, "A microbiological study of neonatal conjunctivae and conjunctivitis," *British Journal of Ophthalmology*, vol. 61, no. 9, 1977, pp. 601-607, doi: 10.1136/bjo.61.9.601.
- [13] M. Gaubatz and R. Ulichney, "Automatic red-eye detection and correction," *Proceedings. International Conference on Image Processing*, 2002, pp. I-I, doi: 10.1109/ICIP.2002.1038147.
- [14] Jian Wan and XuePing Ren, "Automatic red-eyes detection based on AAM," *2004 IEEE International Conference on Systems, Man and Cybernetics (IEEE Cat. No.04CH37583)*, 2004, pp. 6337-6341 vol.7, doi: 10.1109/ICSMC.2004.1401395.
- [15] H. Wang *et al.*, "Early detection and classification of live bacteria using time-lapse coherent imaging and deep learning," *Light: Science & Applications*, vol. 9, no. 1, 2020, pp. 1-17, doi: 10.1038/s41377-020-00358-9.
- [16] Ş. Karahan and Y. S. Akgül, "Eye detection by using deep learning," *2016 24th Signal Processing and Communication Application Conference (SIU)*, 2016, pp. 2145-2148, doi: 10.1109/SIU.2016.7496197.
- [17] S. Hameed and H. M. Ahmed, "Eye diseases classification using back propagation with parabola learning rate," *Al-Qadisiyah Journal Of Pure Science*, vol. 26, no. 1, 2021, pp. 1-9, doi: 10.29350/qjps2021.26.1.1220.
- [18] S. K. Sundararajan and S. P. D., "Detection of Conjunctivitis with Deep Learning Algorithm in Medical Image Processing," *2019 Third International conference on I-SMAC (IoT in Social, Mobile, Analytics and Cloud) (I-SMAC)*, 2019, pp. 714-717, doi: 10.1109/I-SMAC47947.2019.9032705.
- [19] S. Malik, N. Kanwal, M. N. Asghar, M. Ali, I. Karamat, and M. Fleury, "Data driven approach for eye disease classification with machine learning," *Applied Sciences*, vol. 9, no. 14, 2019, p. 2789, doi: 10.3390/app9142789.
- [20] H. Masumoto *et al.*, "Severity classification of conjunctival hyperaemia by deep neural network ensembles," *Journal of ophthalmology*, vol. 2019, 2019, pp. 1-11, doi: 10.1155/2019/7820971.
- [21] M. Manchalwar and K. Warhade, "Detection of cataract and conjunctivitis disease using histogram of oriented gradient," *International Journal of Engineering and Technology (IJET)*, vol. 9, no. 3, pp. 2400-2406, 2017, doi: 10.21817/ijet/2017/v9i3/1709030214.
- [22] L. Jain, H. V. S. Murthy, C. Patel and D. Bansal, "Retinal Eye Disease Detection Using Deep Learning," *2018 Fourteenth International Conference on Information Processing (ICINPRO)*, 2018, pp. 1-6, doi: 10.1109/ICINPRO43533.2018.9096838.
- [23] K. Tsubota, E. Takamura, T. Hasegawa, and T. Kobayashi, "Detection by brush cytology of mast cells and eosinophils in allergic and vernal conjunctivitis," *Cornea*, vol. 10, no. 6, 1991, pp. 525-531, doi: 10.1097/00003226-199111000-00011.
- [24] Y. Dong, Z. Zhang, Z. Qiao and J. Yang, "Classification of cataract fundus image based on deep learning," *2017 IEEE International Conference on Imaging Systems and Techniques (IST)*, 2017, pp. 1-5, doi: 10.1109/IST.2017.8261463.





- [25] M. Gunay, E. Goceri and T. Danisman, "Automated Detection of Adenoviral Conjunctivitis Disease from Facial Images using Machine Learning," *2015 IEEE 14th International Conference on Machine Learning and Applications (ICMLA)*, 2015, pp. 1204-1209, doi: 10.1109/ICMLA.2015.232.
- [26] A. A. Bhadra, M. Jain and S. Shidnal, "Automated detection of eye diseases," *2016 International Conference on Wireless Communications, Signal Processing and Networking (WiSPNET)*, 2016, pp. 1341-1345, doi: 10.1109/WiSPNET.2016.7566355.
- [27] O. Perdomo, J. Arevalo, and F. A. González, "Convolutional network to detect exudates in eye fundus images of diabetic subjects," In *12th International Symposium on Medical Information Processing and Analysis*, vol. 10160, pp. 235-240. SPIE, 2017, doi: 10.1117/12.2256939.
- [28] N. A. El-Hag *et al.*, "Classification of retinal images based on convolutional neural network," *Microscopy Research and Technique*, vol. 84, no. 3, 2021, pp. 394-414, doi: 10.1002/jemt.23596.
- [29] P. Chakraborty, and C. Tharini, "Pneumonia and Eye Disease Detection using Convolutional Neural Networks," *Engineering, Technology & Applied Science Research*, vol. 10, no. 3, 2020, pp. 5769-5774, doi: 10.48084/etasr.3503.
- [30] T. Nazir, A. Irtaza, and V. Starovoitov, "Optic Disc and Optic Cup Segmentation for Glaucoma Detection from Blur Retinal Images Using Improved Mask-RCNN," *International Journal of Optics*, vol. 2021, 2021, doi: 10.1155/2021/6641980.
- [31] M. S. A. Vigil, M. M. Barhanpurkar, N. R. Anand, Y. Soni and A. Anand, "EYE SPY Face Detection and Identification using YOLO," *2019 International Conference on Smart Systems and Inventive Technology (ICSSIT)*, 2019, pp. 105-110, doi: 10.1109/ICSSIT46314.2019.8987830.
- [32] K. Prasad, P. S. Sajith, M. Neema, L. Madhu and P. N. Priya, "Multiple eye disease detection using Deep Neural Network," *TENCON 2019 - 2019 IEEE Region 10 Conference (TENCON)*, 2019, pp. 2148-2153, doi: 10.1109/TENCON.2019.8929666.
- [33] A. K. Nsaif *et al.*, "FRCNN-GNB: Cascade Faster R-CNN With Gabor Filters and Naïve Bayes for Enhanced Eye Detection," in *IEEE Access*, vol. 9, pp. 15708-15719, 2021, doi: 10.1109/ACCESS.2021.3052851.
- [34] A. Halevy, P. Norvig, and F. Pereira, "The unreasonable effectiveness of data," *IEEE intelligent systems*, vol. 24, no. 2, 2009, pp. 8-12, doi: 10.1109/MIS.2009.36.
- [35] Md. H. I. Bijoy, S. A. Akhi, Md. A. A. Nayeem, Md M. Rahman, and Md J. Mia, "Prediction of internet user satisfaction levels in Bangladesh using data mining and analysis of influential factors," *Bulletin of Electrical Engineering and Informatics*, vol. 11, no. 2, 2022, pp. 926-935, doi: 10.11591/eei.v11i2.3617.
- [36] J. Mia, H. I. Bijoy, S. Uddin and D. M. Raza, "Real-Time Herb Leaves Localization and Classification Using YOLO," *2021 12th International Conference on Computing Communication and Networking Technologies (ICCCNT)*, 2021, pp. 1-7, doi: 10.1109/ICCCNT51525.2021.9579718.
- [37] F. J. M. Shamrat *et al.*, "Analysing most efficient deep learning model to detect COVID-19 from computer tomography images," *Indonesian Journal of Electrical Engineering and Computer Science*, vol. 26, no. 1, 2022, pp. 462-471, doi: 10.11591/ijeecs.v26.i1.pp462-471.

BIOGRAPHIES OF AUTHORS



Abu Kowshir Bitto     received his undergraduate degree in Software Engineering Major in Data Science at Daffodil International University (DIU), Dhaka, Bangladesh. He is currently attending MediprospectsAI as a Research and Development Engineer. He is a chief human resource executive (CHRE) at Virtual Multisidisciplinary Research Lab. He previously worked as a Research Assistant at the Data Science Lab DIU. His research experience and interest now in computer vision, data science, and natural language processing. He can be contacted at email: abu.kowshir777@gmail.com.



Dr. Imran Mahmud     is an associate professor and head of the Department of Software Engineering (SWE) at Daffodil International University. He is also an adjunct professor at the Graduate School of Business, Universiti Sains Malaysia. Dr. Imran is an expert in business analytics, technology management, and structural equation modeling. He can be contacted at email: imranmahmud@daffodilvarsity.edu.bd.